Materials Transactions, Vol. 57, No. 10 (2016) pp. 1837 to 1844

Mobility of Twin Boundaries in Fe-Pd-Based Ferromagnetic Shape Memory Alloys

Federico Guillermo Bonifacich[1], Osvaldo Agustín Lambri[1,*], José Ignacio Pérez-Landazábal[2,3], Damián Gargicevich[1], Vicente Recarte[2,3] and Vicente Sánchez-Alarcos[2,3]

[1]*CONICET-UNR, Laboratorio de Materiales, Escuela de Ingeniería Eléctrica, Centro de Tecnología e Investigación Eléctrica, Facultad de Ciencias Exactas, Ingeniería y Agrimensura, Avda. Pellegrini 250, (2000) Rosario, Argentina*
[2]*Departamento de Física, Universidad Pública de Navarra, Campus de Arrosadía, 31006 Pamplona, Spain*
[3]*Institute for Advanced Materials (INAMAT), Universidad Pública de Navarra, Campus de Arrosadía, 31006 Pamplona, Spain*

The mobility of twin boundaries in (at.%) $Fe_{70}Pd_{30}$, $Fe_{67}Pd_{30}Co_3$ and $Fe_{66.8}Pd_{30.7}Mn_{2.5}$ has been studied by mechanical spectroscopy. Measurements were carried out in amplitude dependent damping regime. A new model based on the Friedel theory was developed to obtain the activation energy (~2 kJ/mol) for twin boundaries motion. The model describes the amplitude dependent damping from thermally assisted break-away of dislocations. Interaction processes among twin boundaries, dislocations and vacancies during the recovery of the structure are also discussed. Moreover, a damping peak related to a dislocation dragging mechanism controlled by vacancies migration without break-away, earlier reported in Fe-Pd alloys, was also found in Fe-Pd-Co and Fe-Pd-Mn alloys. [doi:10.2320/matertrans.M2016243]

(Received July 1, 2016; Accepted July 27, 2016; Published September 25, 2016)

Keywords: *iron-palladium based alloys, ferromagnetic shape memory alloys, martensitic transformation, twin boundary, damping*

1. Introduction

Fe-Pd alloys with compositions close to $Fe_{70}Pd_{30}$ show the best mechanical properties among ferromagnetic shape memory alloys (FSMA) as well as induced strains due to redistribution of variants under magnetic fields or mechanical stresses.[1–6] In FSMA the mobility of twin boundaries is an important factor affecting the magnetic field or stress induced strain.[5–7] However, there are scarce works regarding the determination of the activation energies involved in the variants movement.

Mechanical spectroscopy is a very sensitive technique used to analyse defects interaction processes in materials and phase transformations and in particular it has been widely applied to study the martensitic transition (MT), see for instance Refs. 8–14). Amplitude dependent damping (ADD) studies are related to the motion of linear/planar defects and therefore it is an efficient tool to study pinning-related and interaction phenomena.[8,14,15] ADD behaviour in shape memory alloys is usually ascribed to stress-induced rearrangement of the material, resulting in variant-boundary motion, variant-boundaries interaction with defects or both. This type of hysteretic behaviour is not different from that described by Granato-Lücke[16] in terms of dislocation break away.[14,17]

Cu-Al-Ni[18], Ni-Mn-Cu[19] and Mn-Cu[20] show a relaxation peak related to the variants movement and in these cases the activation energy can be determined from the frequency dependence of the peak temperature. In contrast, in Ni_2MnGa, where a relaxation peak related to variants movement could not be found, Gavriljuk *et. al.*[7] calculated its activation energy considering the ADD promoted by a frictional process related to the swept area of the variant. The swept area was proposed to increase with the reciprocal of the exponential temperature[7] in parallel to the expression used to determine the interaction energy between dislocations and pinning points in the Granato-Lücke model.[16,17,21,22]

The activation energy for variants movement in Fe-Pd based alloys has not been reported in the literature. Consequently, the aim of this work is to determine the interaction energy involved in the movement of variants in Fe-Pd, Fe-Pd-Co and Fe-Pd-Mn FSMA. Due to the appearance of the irreversible phase, it is not possible to extend the temperature range below room temperature to find a relaxation peak related to the movement of variants, so ADD studies were used in the present work. Nevertheless, the model of Gavriljuk *et. al.*[7] cannot be applied in Fe-Pd based FSMA since the damping values and the strength of ADD, decrease with a temperature increase.[13] Therefore, a new model based on the Friedel theory[22] to describe the ADD has been developed. In addition, the relaxation peak related to the interaction of dislocations with vacancies already reported in Fe-Pd alloys[13] has been also found in Fe-Pd-Co and Fe-Pd-Mn alloys.

2. Theoretical Background, the Friedel Model for ADD

According to the Friedel[22] model, if a small stress σ is suddenly applied to a dislocation line, the probability of unpinning from an impurity is given by

$$\frac{\upsilon b}{\lambda}\exp\left(-\frac{|E_M| - (\sigma - \sigma_i)bd\lambda}{kT}\right) \quad (1)$$

where: υ is the atomic frequency, λ is the loops length, σ_i is a frictional Peierls-Nabarro stress, d ≈ b, the width of the dislocation and E_M is the binding free energy between impurities and dislocations.

If there are $N_0 \approx l^{-3}$ (l being the dislocation length) dislocations loops in the metal, the total number of loops unpinned after a time $1/2\upsilon_0$ is

$$N = \frac{\upsilon b}{2\upsilon_0\lambda}N_0\exp\left(-\frac{|E_M| - (\sigma - \sigma_i)bd\lambda}{kT}\right) \quad (2)$$

Assuming a sinusoidal stress and taking in account the relation between the dislocation strain and the quantity of dislocations sweeping a given area, Friedel finds the following equation to describe ADD as a function of both, temperature and strain,

*Corresponding author, E-mail: olambri@fceia.unr.edu.ar

$$Q^{-1} = \frac{\Delta W}{W} = \frac{1}{20}\frac{\upsilon b}{\upsilon_0 \lambda} N_0 \exp\left(-\frac{|E_M| - (\sigma - \sigma_i) b d \lambda}{kT}\right) \quad (3)$$

where ΔW and W are the lost energy per cycle and the stored energy at the peak of the cycle, respectively.

By writing the stress as a function of strain, ε, such that

$$\sigma = \mu\varepsilon \text{ and } \sigma_i = \mu\varepsilon_{ch}, \quad (4)$$

where μ is the shear modulus and ε_{ch} is a characteristic strain for the Peierls-Nabarro stress, and replacing eqs. (4) in eq. (3), it can be easily shown that

$$\ln Q^{-1} = A(T) + B(T)\varepsilon \quad (5)$$

Thus, at constant temperature, a linear relationship between the natural logarithm of damping and strain must be observed. This representation is the so called Friedel plot.

3. Experimental

Polycrystalline ingots of nominal composition (at.%) $Fe_{70}Pd_{30}$, $Fe_{67}Pd_{30}Co_3$, $Fe_{66.8}Pd_{30.7}Mn_{2.5}$ were prepared from high purity elements by arc melting under protective Ar atmosphere. The ingots were homogenized in vacuum quartz ampoules at 1273 K during 24 hours. In order to retain the disordered γ(Fe, Pd) cubic structure where the MT occurs, the ingots were annealed at 1173 K during 30 minutes and then quenched into iced water. The composition of the quenched alloys was analyzed by energy dispersive X-ray spectroscopy (EDS) in a Jeol JSM-5610LV Scanning Electron Microscope (SEM).

In order to determine the transformation temperatures, differential scanning calorimetry (DSC) measurements were carried out at a heating/cooling rate of 10 K/min in a TA Q100 calorimeter under nitrogen protective atmosphere.

Mechanical spectroscopy (MS), referred to as the internal friction method in the early literature, involves the simultaneous measurement of damping, Q^{-1} (or internal friction) and natural frequency (f, f^2 being proportional to the elastic modulus) as a function of temperature and/or strain.[17,21,23,24] Measurements were performed in a mechanical spectrometer based on an inverted torsion pendulum under Ar at atmospheric pressure. The maximum strain on the sample surface was 5×10^{-5}. The measurement frequency was around 1 Hz (except for measurements performed to obtain the activation energy of the relaxation processes). The heating and cooling rates employed in the tests were 1 K/minute. Samples were also measured under a H_{DC} = 40 kA/m direct magnetic field. The magnetic field was produced by a water cooled coil parallel to the torsion axis.

Amplitude dependent damping (ADD), i.e. damping as a function of the maximum strain on the sample, ε_0, was calculated from eq. (6).[25–27]

$$Q^{-1}(\varepsilon_0) = -\frac{1}{\pi}\frac{d(\ln(A_n))}{dn} \quad (6)$$

where A_n is the area of the n^{th} decaying sinusoidal oscillation and n is the period number. The period number depends on the time and resonance frequency. The time dependence of the amplitude (see upper inset in the Fig. 1) can be used to determine the logarithm of the decaying areas as a function of the period number, see Fig. 1. A magnification of a zone of the decaying oscillations is also shown in the lower inset, where two consecutive areas are depicted. The use of the decaying areas is equivalent to the use of decaying semi-amplitudes, but with a better signal to noise ratio[25,28,29]. The decaying of the oscillations were performed at constant temperature (T ± 0.5 K) and polynomials were used to analyse the curves by Chi-square fitting (see Fig. 1). Subsequently the eq. (6) was applied. Polynomials of degree higher than 1 indicate that Q^{-1} is a function of ε_0, leading to the appearance of ADD effects, as it can be inferred easily. In fact, the derivative of a polynomial of degree 1 gives a constant, so the damping is not amplitude dependent (see eq. (6)). In addition, if non linear effects appear, i.e. doubling the stress does not lead to doubling strain and the logarithm of the decaying oscillations does not exhibit linear behaviour. Indeed, the contribution to the measured damping from different parts of the samples will be different due to the spatial inhomogeneity of the strain field under torsional oscillations leading to an amplitude dependent damping[25,30,31]. This procedure allows to obtain damping as a function of the maximum strain on the sample (ε_0) from free decaying oscillations.[25–27] The strength of the amplitude dependent damping behaviour (ADD), can be determined through the average slope of the $Q^{-1}(\varepsilon_0)$ curve using the S coefficient:[13,25–27]

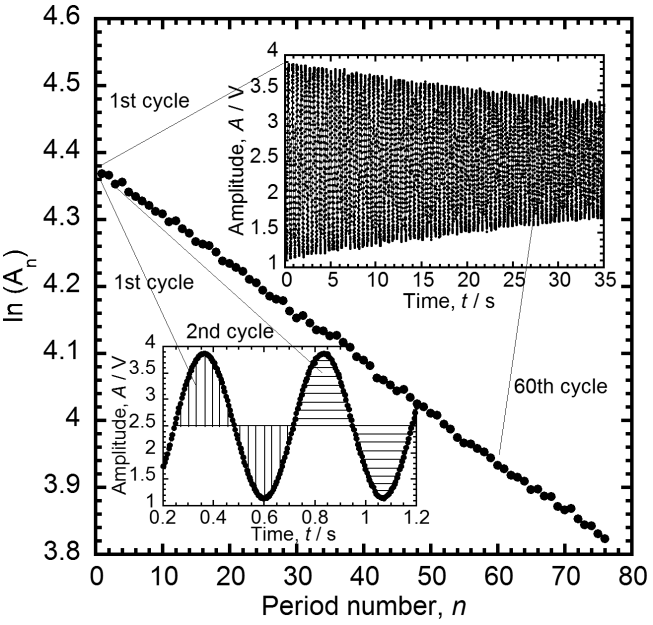

Fig. 1 Logarithm of the decaying areas ($\ln(A_n)$) as a function of the period number (n). Upper inset: oscillation decay. Lower inset: magnification of the oscillation decay showing the first and second decaying areas.

$$S = \frac{\Delta Q^{-1}}{\Delta \varepsilon_0} \quad (7)$$

where ΔQ^{-1} is the damping change corresponding to the full amplitude changes $\Delta\varepsilon_0$ measured in the whole oscillating strain range. Depending both on the oscillating strain level (usually higher than 10^{-6}) and on the measuring temperature, the damping can be either amplitude independent or amplitude dependent. ADD is usually a consequence of interaction processes involving mobile dislocations through thermally

activated mechanisms. The thermally assisted break-away of dislocations from weak pinning points is one of such examples. Mechanisms involving the dragging of jogs by screw dislocations, or the pinning by large precipitates or other blocked dislocations lead to nearly amplitude independent damping processes.[13,14,22)]

4. Results and Discussion

Figure 2 shows the DSC thermograms during heating and cooling corresponding to Fe-Pd, Fe-Pd-Co and Fe-Pd-Mn alloys. The maximum temperature achieved during heating was 603 K in all cases. The MT occurs at 290 K, 250 K and 310 K respectively. On the other side, the Curie temperature, Tc, can be observed at 560 K, 600 K, 525 K. Finally, the transformation enthalpies corresponding to Fe-Pd, Fe-Pd-Co and Fe-Pd-Mn are 0.8 J/g, 0.7 J/g and 0.8 J/g, respectively.[13,32,33)] In addition, precipitation processes can be neglected in the studied temperature range.

Figure 3 shows some curves of damping against maximum strain amplitude at different constant temperatures, during the first and the second warm-ups in a Fe-Pd alloy. Damping curves as a function of temperature for different strain can be obtained using the intersection between these curves and a vertical line located at a particular strain (ε_0) value.[26)] Figure 4 has been obtained following this procedure for the first and the second warming runs. Indeed, Figs. 4(a) to 4(c) show

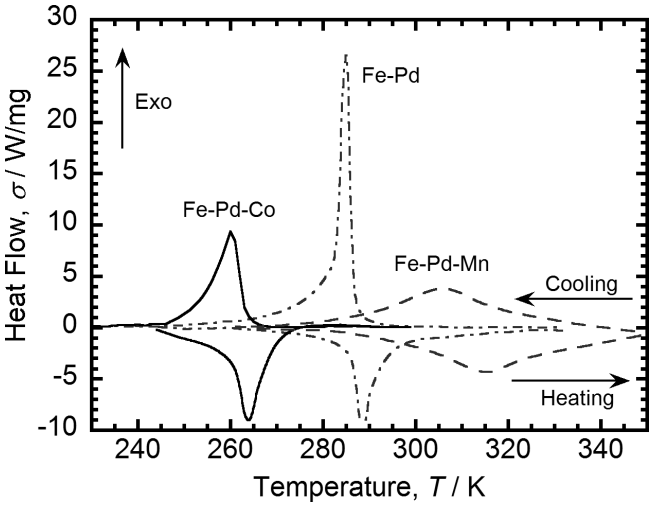

Fig. 2 DSC thermograms for Fe-Pd (dotted-dashed line), Fe-Pd-Co (full line), Fe-Pd-Mn (dashed line).

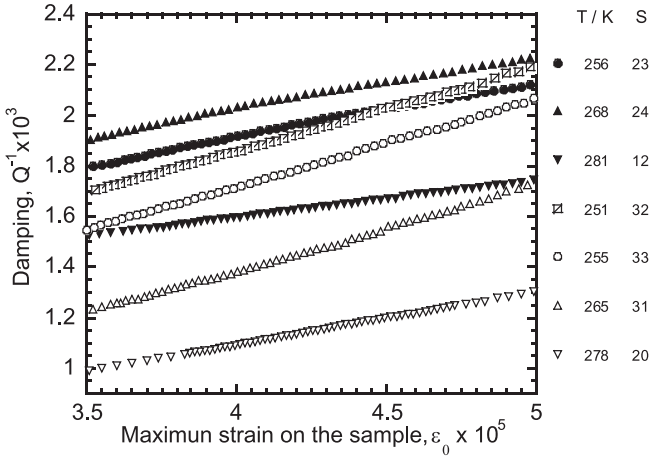

Fig. 3 Damping as a function of strain amplitude at different constant temperatures, during the first (full symbols) and the second (empty symbols) warming runs (Fe-Pd sample). The calculated S parameters are also shown on the right column.

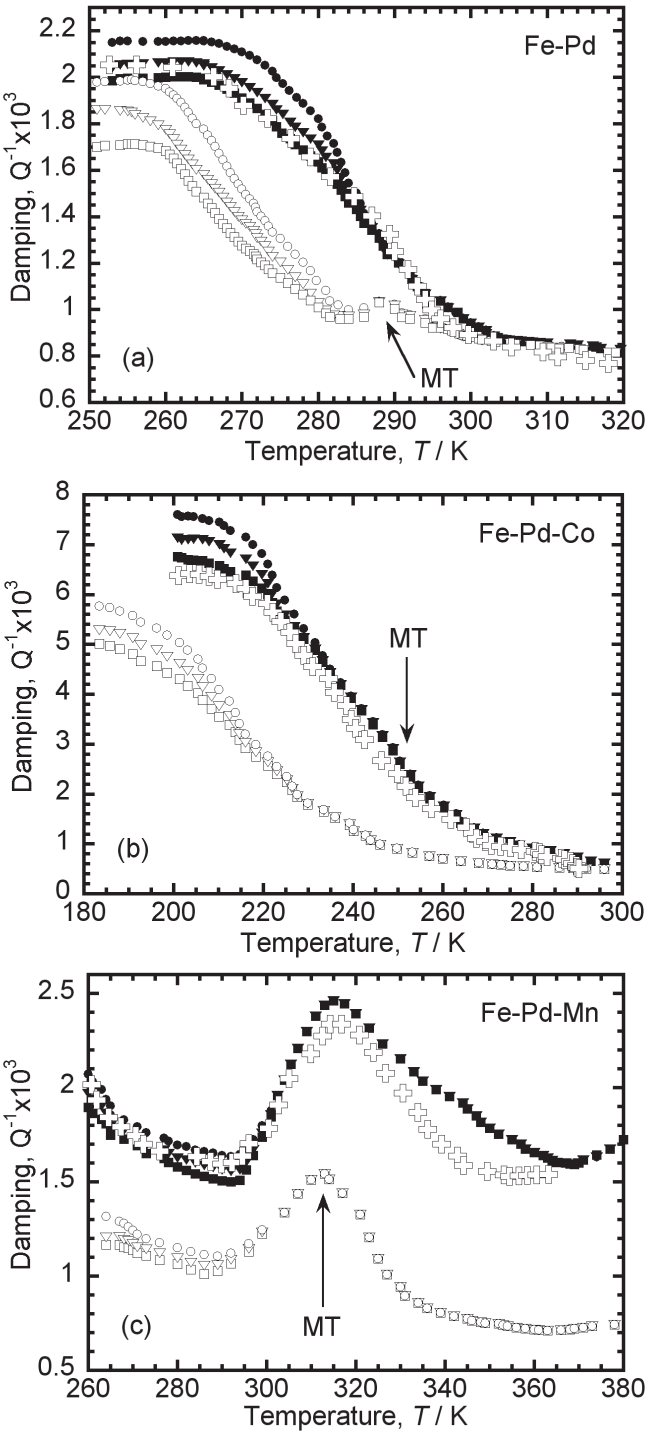

Fig. 4 Amplitude dependent damping curves in the zone of the martensitic phase (Circles: 5×10^{-5}, Inverted Triangles: 4×10^{-5}, Squares: 3.5×10^{-5}). Full symbols: 1st warming without magnetic field. Empty symbols: 2nd warming without magnetic field. Crosses: Amplitude dependent damping measured during the first warming under magnetic field. (a) Fe-Pd, (b) Fe-Pd-Co, (c) Fe-Pd-Mn. MT and the arrow in the figures mean the temperature of martensitic transition.

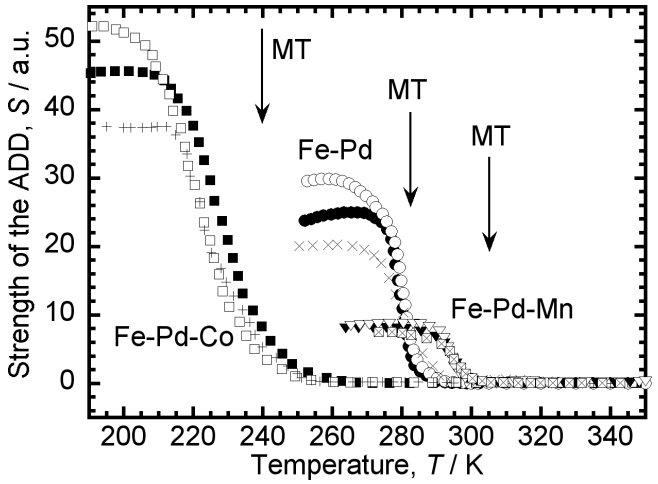

Fig. 5 Strength of the amplitude dependent damping (S) for Fe-Pd, Fe-Pd-Co and Fe-Pd-Mn alloys. Full symbols: 1st warming run without magnetic field. Empty symbols: 2nd warming without magnetic field. Circles: Fe-Pd, Squares: Fe-Pd-Co, Inverted Triangles: Fe-Pd-Mn. Crosses: Amplitude dependent damping measured during the first warming under magnetic field for each alloy. Arrows indicate the temperature for the martensitic transition for each alloy.

the damping around the MT in two consecutive heating runs to 600 K for Fe-Pd, Fe-Pd-Co and Fe-Pd-Mn alloys and for three different maximum oscillating strains (ε_0), to evince the effect of the annealing. An evolution of defects, e.g. recovery, should be expected. The starting measuring temperature is always above the critical temperature where the irreversible bct phase develops,[5,13] so the alloys are free of the irreversible phase. According to the measurements, the damping is amplitude dependent in the fct martensitic region, but independent of the oscillation amplitude above the MT temperature; which is in agreement with previous works.[13,34] In addition, during the second warming the damping values below MT are smaller than those measured during the first warming independently of the alloy or amplitude. For Fe-Pd alloy a small peak related to the MT can be seen at around 290 K during the second warming, while a hump can be appreciated at this temperature during the first warming. On the other side, the MT in Fe-Pd-Co appears as a small hump over the damping curve at around 240 K–250 K. It seems that during the second warming, a peak can be resolved at around 240 K. Finally, for Fe-Pd-Mn the damping peak related to MT can be clearly resolved, exhibiting a smaller dependence on the amplitude of oscillation than for Fe-Pd and Fe-Pd-Co alloys.

The behaviour of the damping curves measured under magnetic field, in another sample taken from the same ingot, during a first warming at maximum strain $\varepsilon_0 = 5 \times 10^{-5}$, is similar to that measured without field in the same conditions but the damping in all alloys is smaller, see Fig. 4.

The strength of the amplitude dependent damping as a function of temperature was determined through the behaviour of the S parameter, see eq. (7), Section 3. Figure 5 summarizes the behaviour of S as a function of temperature for the three studied alloys. Indeed, S decreases as the temperature increases for the three alloys. Above the MT the damping becomes amplitude independent in all alloys. In addition, the higher values of S after the first warming indicate that both the dislocations and variants increase their mobility after annealing. The smallest values of S in the martensitic zones were measured for the Fe-Pd-Mn. These small S values can be a consequence of the presence of small precipitates that appear after quenching.[32] In contrast, the largest S values were measured in Fe-Pd-Co alloy, being this difference controlled probably by the small size of Co atoms regarding the Pd and Mn. The small size of Co could provide room to decrease the internal stresses enhancing the mobility of variants and dislocations.

For Fe-Pd, Fe-Pd-Co and Fe-Pd-Mn the application of a direct magnetic field leads to a decrease both in the damping and S values. The decrease in the values of damping under a direct field in ferromagnetic alloys has been largely studied and it is well established in the literature.[17,21,24,30,35,36] Indeed the magnetic field impedes the movement of the well oriented domain walls, suppressing the so called magnetomechanical damping. The magnetic field leads to a decrease in the mobility of the domain walls, which are at the same time the twin boundaries between martensite variants,[6,7,37] giving rise to a decrease in both the damping and S values within the martensitic region, see Figs. 4 and 5. The main microstructural difference between austenite and martensite is the appearance of crystallographic domains, variants, in the low temperature phase. Therefore, the damping in the martensitic zone and its ADD behaviour could be mainly ascribed to the contribution related to the movement of variants. Other sources of ADD damping in this zone could be also acting overlapped such that, interaction processes among variants, dislocations, vacancies and obstacles.

In order to determine the activation energy controlling the twin boundaries motion, the Friedel model for thermally assisted break away of dislocations from pinning points described in Section 2, will be applied. In fact, the movement of the twin boundary is assumed to be as a line moving in a viscous media, so the Friedel model could be applied if eq. (5) is accomplished. The Friedel plots for some temperatures below the MT for the three studied alloys are shown in Fig. 6. It should be highlighted a good agreement in all cases.

By replacing eq. (4) into eq. (3) the following equation can be obtained:[25]

$$S = \frac{dQ^{-1}}{d\varepsilon} = \frac{1}{20}\frac{\upsilon\mu b^3}{\upsilon_0 kT} N_0 \exp\left(-\frac{|E_M|}{kT}\right) \tag{8}$$

The activation energy E_M can be easily obtained from eq. (8) by taking logarithm, such that

$$\ln\frac{ST}{f^2} = \ln C - \frac{|E_M|}{kT} \tag{9}$$

where $C = \frac{1}{20}\frac{\upsilon b^3 SF}{\upsilon_0 k} \approx$ constant in a restricted temperature range and SF is the proportionality factor between the square oscillating frequency and the elastic modulus,[13,31] which depends on the shape of the sample ($\mu = SF\, f^2$).

Figure 7 shows the plots corresponding to eq. (9) for the first and second heating runs in measurements performed with and without magnetic field. The obtained activation energies for variants movement, E_M, determined from the slope of curves, are listed in Table 1. The written values are the average obtained between two different samples.

The calculated values of E_M, in the present work, are close to those obtained in Ni_2MnGa alloys (1.9–3.8 kJ/mol) by

Gavriljuk *et. al.*[7] Indeed, due to the highly glissile movement of twin boundaries very small values of activation energies should be expected,[6,7,38,39] i.e. the energy saddle point to be overcome by the atoms movements during twining is very small.[6,7,38–40] In addition, an activation energy between 2.2 and 3.3 kJ/mol was obtained applying the procedure developed in the present work to the experimental data earlier reported by Gavriljuk *et. al.*, which is in agreement with their reported values.

It should be pointed out that, the small value of the activation energy obtained in the present work, allows us to re-confirm that the physical mechanism giving rise to amplitude dependent damping is related to the movement of twin boundaries in Fe-Pd based FSMA. In fact, damping mechanisms involving dislocations relaxation processes in iron and in bcc and fcc metals at low temperatures are developed with activation energies higher than 6.2 kJ/mol.[41–48] The lowest activation energy was reported for the kink pair formation in non-screw dislocations in tungsten (α' relaxation, 6.2 kJ/mol).[44] In addition, dislocation relaxation processes give rise to damping peaks as a function of temperature depending on the oscillating frequency, but in the present study on FSMA, relaxation peaks within the martensitic phase were not detected.

Despite the error bandwidths obtained for E_M, a trend can be seen in Fig. 7 and Table 1: The activation energy is the largest in Fe-Pd-Mn alloys and the smallest in Fe-Pd-Co alloys. Moreover, during the second warming, the activation energy for the migration of variants decreases. On the other side, measurements performed under magnetic field, exhibits higher values of E_M. The decrease in the values of E_M after annealing up to 603 K could be related to the increase in the

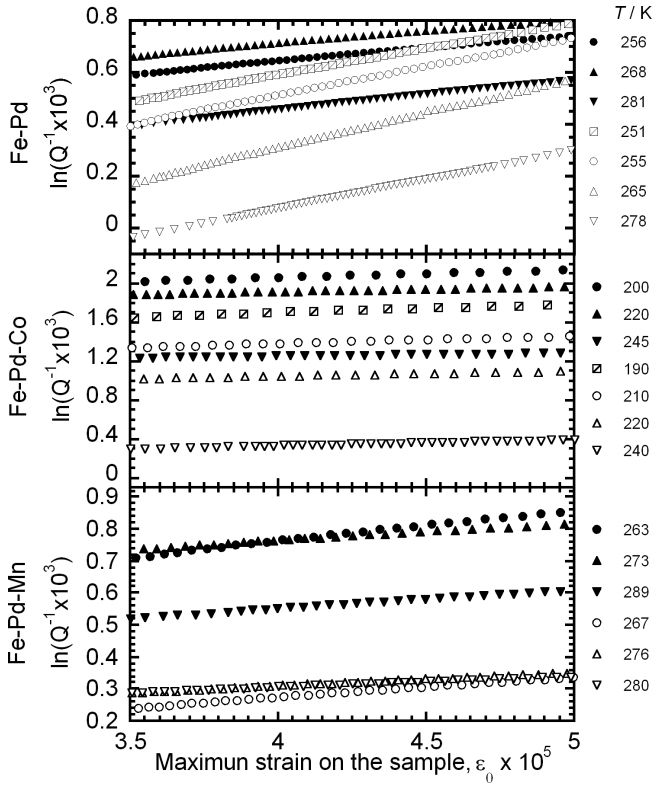

Fig. 6 Friedel plots, eq. (5), for Fe-Pd (upper plot), Fe-Pd-Co (middle plot) and Fe-Pd-Mn (lower plot). Full symbols: 1st warming run without magnetic field. Empty symbols: 2nd warming without magnetic field.

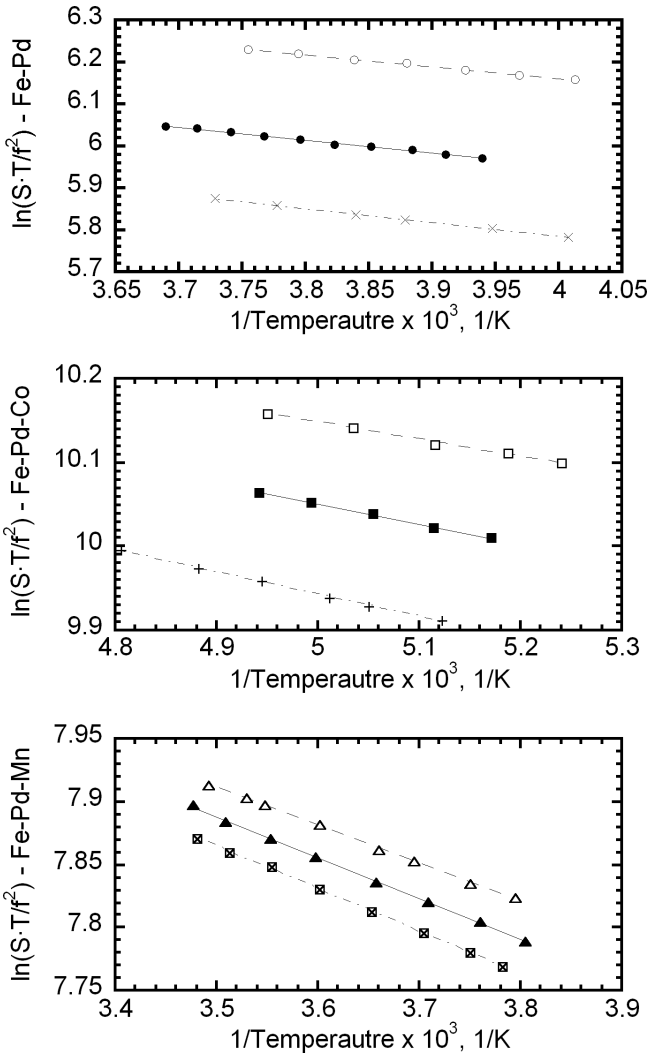

Fig. 7 Representation of eq. (9) from the new model for obtaining the activation energy for the movement of twin boundaries. Fe-Pd: upper plot, Fe-Pd-Co: middle plot and Fe-Pd-Mn: lower plot. Full symbols: 1st warming run without magnetic field. Empty symbols: 2nd warming without magnetic field. Crosses: Amplitude dependent damping measured during the first warming under magnetic field.

Table 1 Activation energy for the movement of twin boundaries, E_M, calculated by means of eq. (9) for the first and second warming runs without magnetic field. The values during the first warming under magnetic field are also listed. Written values are the average between two samples.

	E_M (kJ/mol) Fe-Pd	E_M (kJ/mol) Fe-Pd-Co	E_M (kJ/mol) Fe-Pd-Mn
1st warming run without H_{DC}	2.5 ± 0.2	2.0 ± 0.3	2.7 ± 0.1
2nd warming run without H_{DC}	2.3 ± 0.1	1.7 ± 0.2	2.5 ± 0.2
1st warming run with H_{DC}	2.7 ± 0.1	2.3 ± 0.3	2.8 ± 0.1

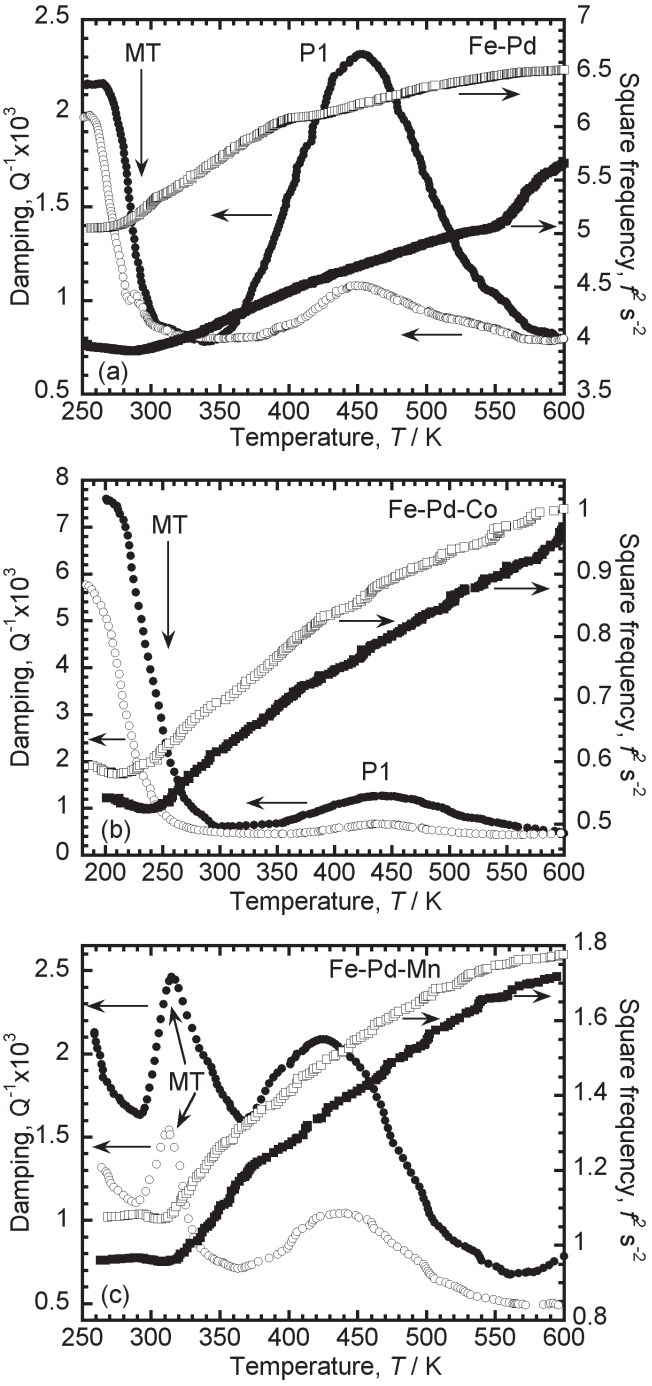

Fig. 8 Damping (circles) and square frequency (squares, proportional to the elastic modulus) measured during warming in the whole temperature range, at $\varepsilon_0 = 5 \times 10^{-5}$. (a) Fe-Pd, (b) Fe-Pd-Co, (c) Fe-Pd-Mn. Full symbols: 1st warming run without magnetic field. Empty symbols: 2nd warming without magnetic field. Vertical arrows indicate the martensitic transition temperature.

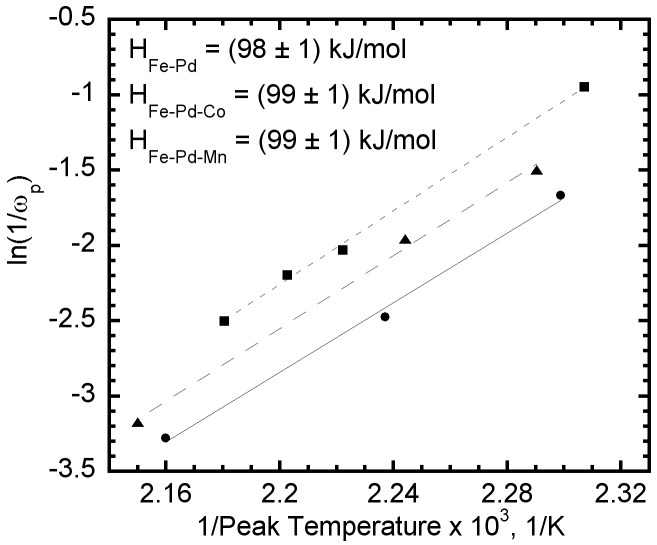

Fig. 9 Arrhenius plots for the studied alloys. T_p and ω_p are the temperature and the circular frequency ($\omega = 2\,\pi$ f) evaluated at the maximum of the damping peak.

mobility of dislocations and variants, as it is shown by the increase in the S values during the second warming run. In order to study the recovery processes of the quenched-in-defects by annealing up to 603 K, the response of the MS test at temperatures above the MT will be studied in the followings paragraphs.

Figures 8(a) to 8(c) show the behaviour of the damping for a maximum strain $\varepsilon_0 = 5 \times 10^{-5}$, during two consecutive warming runs in a wider temperature range for Fe-Pd, Fe-Pd-Co and Fe-Pd-Mn alloys, respectively. In all cases, a damping peak at around 430–450 K, called hereafter P1, (nomenclature used in previous works[13]) can be observed. The physical mechanism responsible of the P1 relaxation peak in Fe-Pd alloys was proposed to be a dislocation dragging controlled by the migration of vacancies without break-away.[13] The Figures also show the behaviour of the square frequency (which is proportional to the elastic modulus) as a function of temperature, for two consecutive warming runs. The inverse modulus temperature dependence, i.e. the increase in the modulus values as the temperature increases was explained through a mechanism controlled by the dragging of point defects by the dislocation during their movement.[13] In addition, the decrease in the peak height for P1 and the increase in the modulus values, after the first warming up to 603 K for Fe-Pd; were previously related to the recovery of the structure leading to a decrease in the amount of quenched-in-defects such as vacancies and dislocations.[13]

To analyze the relaxation peaks for Fe-Pd-Co and Fe-Pd-Mn in more detail, the activation energies (H) and pre-exponential factors (τ_0) of the relaxation time, determined from the Arrhenius plot in Fig. 9, (shifting of the peak temperature with an increase in frequency) are detailed in Table 2 for the three different alloys. In summary, the similar values found for H among Fe-Pd[13] and Fe-Pd-Co and Fe-Pd-Mn indicate that in the three alloys systems this peak has the same physical origin that is, a dislocation dragging mechanism controlled by the migration of vacancies without break-away.[13]

Then, the decrease in the peak height of P1 during the second warming (see Fig. 8) for Fe-Pd, Fe-Pd-Co and Fe-Pd-Mn, indicates that a recovery of the structure, during the first warming run, takes place leading to a decrease in the amount of quenched-in-dislocations and –vacancies. Indeed, a less amount of interacting dislocations and vacancies decreases the strength of P1 peak.[15,17] In addition, the higher values of S for the annealed samples shown in Fig. 5 reveals an increase in the dislocations and variants mobility promoted by the recovery of the structure. Therefore, the decrease in

Table 2 Activation energy (H) and pre-exponential factor (τ_0) of the relaxation time for P1 peak in the three studied alloys.

Alloy/Activation parameters	Fe-Pd	Fe-Pd-Co	Fe-Pd-Mn
H (kJ/mol)	98 ± 1	99 ± 1	99 ± 1
τ_0 (s)	$5 \times 10^{-(13 \pm 0.5)}$	$2 \times 10^{-(13 \pm 0.5)}$	$3 \times 10^{-(13 \pm 0.5)}$

the values of E_M after the first warming (see Table 1) can be related to the decrease in the amount of quenched-in-dislocations and –vacancies, which enhance the mobility of twin boundaries. In fact, a decrease of quenched-in-defects, leads to a decrease in the amount of obstacles to be overcome by the twin boundaries. In contrast, S shows smaller values under magnetic field (as-quenched alloys), due to a decrease in the mobility of twin boundaries as a consequence of the interaction with the magnetic domain walls. Consequently, the activation energy calculated for the movement of variants in quenched samples under magnetic field are the highest.

The decrease in the amount of dislocations and vacancies after the first warming, allows to explain the decrease in the damping in the martensitic zone during the second warming; by considering dragging processes of defects. A decrease in the amount of quenched-in-dislocations and vacancies to be dragged leads to a reduction in the values of martensitic damping controlled by dragging.[49,50)]

5. Conclusions

The amplitude dependent damping behaviour exhibited by Fe-Pd, Fe-Pd-Co and Fe-Pd-Mn alloys has been successfully described by a model based on the Friedel theory addressed to the amplitude dependent damping phenomenon promoted by the thermally assisted break-away of dislocations from pinning points. The formalism was applied successfully to obtain the activation energy corresponding to the movement of twin boundaries. The model carried out in the present work is very useful when the strength of the amplitude dependent damping decreases as the temperature increases and when a damping peak related to the movement of twin boundaries cannot be found. An activation energy close to 2 kJ/mol was found for Fe-Pd based FSMA. The activation energy decreases after annealing the sample indicating that the movement of the twin boundaries is sensitive to dislocations and vacancies. Dragging of vacancies and dislocations by twin boundaries during their movement can be inferred. Moreover, the appearance of the damping peak at around 430–450 K, in the austenite phase, related to the dislocation dragging mechanism controlled by the migration of vacancies without break-away earlier reported for Fe-Pd alloys was determined in Fe-Pd-Co and Fe-Pd-Mn alloys.

Acknowledgements

This work was partially supported by the CONICET-PIP No. 179CO, the Spanish "Ministerio de Economía y Competitividad" (Projects number MAT2015-65165-C2-1-R), the PID-UNR ING 450 and ING 453 (2014–2017) and the Collaboration Agreement between the Universidad Pública de Navarra and the Universidad Nacional de Rosario, Res. 3247/2015. O.A.L wishes to acknowledge to Rev. P. Ignacio Peries for everything.

REFERENCES

1) M. Sugiyama, R. Oshima and F.E. Fujita: Trans. JIM **19** (1984) 585–592.
2) M. Sugiyama, R. Oshima and F.E. Fujita: Trans. JIM **27** (1986) 719–730.
3) R.D. James and M. Wuttig: Philos. Mag. A **77** (1998) 1273–1299.
4) T. Kakeshita, T. Fukuda and T. Takeuchi: Mater. Sci. Eng. A **438–440** (2006) 12–17.
5) V. Sánchez-Alarcos, J.I. Pérez-Landazábal and V. Recarte: Mater. Sci. Forum **635** (2010) 103–110.
6) D. C. Lagoudas (ed): *Shape Memory Alloys, Modeling and Engineering Applications* (Springer, New York, 2007).
7) V.G. Gavriljuk, O. Söderberg, V.V. Bliznuk, N.I. Glavatska and V.K. Lindroos: Scr. Mater. **49** (2003) 803–809.
8) E. Cesari, S. Kustov, S. Golyandin, K. Sapozhnikov and J. Van Humbeeck: Mater. Sci. Eng. A **438–440** (2006) 369–373.
9) E. Cesari, V.A. Chernenko, V.V. Kokorin, J. Pons and C. Segui: Acta Mater. **45** (1997) 999–1004.
10) V.A. Chernenko, C. Segui, E. Cesari, J. Pons and V.V. Kokorin: Phys. Rev. B **57** (1998) 2659–2662.
11) S. Kustov and J. Van Humbeeck: Mater. Sci. Forum **583** (2008) 85–109.
12) S. Kustov, S. Golyandin, K. Sapozhnikov, E. Cesari, J. Van Humbeeck and R. De Batist: Acta Mater. **50** (2002) 3023–3044.
13) J.I. Pérez-Landazábal, O.A. Lambri, F.G. Bonifacich, V. Sánchez-Alarcos, V. Recarte and F. Tarditti: Acta Mater. **86** (2015) 110–117.
14) R. De Batist: *Mechanical spectroscopy*, ed. by E. Lifshin: Characterization of Materials ed. by R. W. Cahn, P. Haasen and E. J. Kramer: Materials Science and Technology, 2B, Part II (VCH, Weinheim, 1991).
15) J. Van Humbeeck: *High damping capacity due to microstructural interfaces* ed. by B.B. Rath and M.S. Misra: *Role of Interfaces on Materials Damping* (Proc. ASM's Materials Week and TMS/AIME Fall Meeting, Toronto, 1985).
16) A. Granato and K. Lücke: J. Appl. Phys. **27** (1956) 583–593.
17) R. Schaller, G. Fantozzi and G. Gremaud (Eds): *Mechanical Spectroscopy* (Trans Tech. Publ Ltd, Switzeland, 2001).
18) K. Suzuki, N. Nakanishi and H. Mitani: J. Japan Inst. Metals **44** (1980) 43–50.
19) F. Yin, K. Nagai, K. Watanabe and K. Kawahara: Mater. Trans. **44** (2003) 1671–1674.
20) F. Yin, T. Sakaguchi, Q. Tian, A. Sakurai and K. Nagai: Mater. Trans. **46** (2005) 2164–2168.
21) A. S. Nowick and B.S. Berry: *Anelastic Relaxation in Crystalline Solids* (Academic Press, New York, 1972).
22) J. Friedel: *Dislocations* (Addison-Wesley, Reading, 1967).
23) D.H. Niblett and J. Wilks: Adv. Phys. **9** (1960) 1–88.
24) C. Zener: *Elasticity and Anelasticity of Metals* (University of Chicago Press, Chicago, 1956).
25) O. A. Lambri: *A review on the problem of measuring nonlinear damping and the obtainment of intrinsic damping* ed. by J. Martinez-Mardones, D. Walgraef and C. H. Wörner: *Materials Instabilities* (World Scientific Publishing, New York, 2000).
26) B.J. Molinas, O.A. Lambri and M. Weller: J. Alloy. Compd. **211–212** (1994) 181–184.
27) G.I. Zelada-Lambri, O.A. Lambri and J.A. García: J. Nucl. Mater. **353** (2006) 127–134.
28) K. Iwasaki: J. Phys. E Sci. Instrum. **16** (1983) 421–426.
29) G. I. Zelada, *Mecanismos de Interacción Dislocaciones-Defectos Puntuales en Molibdeno a Temperaturas entre 300 K - 1300 K (0;3 TF)* (Ph.D. Thesis, Universidad Nacional de Rosario, Argentina, 2008).
30) B. J. Lazan: *Damping of Materials and Members in Structural Mechanics* (Pergamon, London, 1968).
31) C. T. Wang: *Applied Elasticity* (McGraw-Hill, New York, 1953).
32) V. Sánchez-Alarcos, V. Recarte, J.I. Pérez-Landazábal, M.A. González and J.A. Rodríguez-Velamazán: Acta Mater. **57** (2009) 4224–4232.
33) V. Sánchez-Alarcos, V. Recarte, J.I. Pérez-Landazábal, C. Gómez-Polo, V.A. Chernenko and M.A. González: Eur. Phys. J. Spec. Top. **158** (2008) 107–112.

34) F. Xiao, T. Fukuda, T. Kakeshita, M. Jin and X. Jin: J. Alloy. Compd. **649** (2015) 211–215.
35) B. D. Cullity: *Introduction to Magnetic Materials* (Addison-Wesley Publishing Company, London, 1972).
36) R. M. Bozorth: *Ferromagnetism* (Van Nostrand Company, New York, 1951).
37) K. Ullakko: J. Mater. Eng. Perform. **5** (1996) 405–409.
38) R. W. Cahn and P. Haasen: *Physical Metallurgy* (North-Holland, Amsterdam, 1983).
39) T. W. Duerig, K. N. Melton, D. Stöckel and C. M. Wayman: *Engineering Aspects of Shape Memory Alloys* (Butterworth-Heinemann Ltd, London, 1990).
40) K. Otsuka and C. M. Wayman (eds.): *Shape Memory Materials* (Cambridge University Press, Cambridge, 1998).
41) M. Weller, J. Diehl and W. Trifshäuser: Solid State Commun. **17** (1975) 1223–1226.
42) I.G. Ritchie, J.F. Dufresne and P. Moser: Phys. Status Solidi **61** (1980) 591–600 (a).
43) G. Fantozzi and I.G. Ritchie: J de Phys. **42(C5)** (1981) C5–3–C5–23.
44) G.E. Rieu: Acta Metall. **26** (1978) 1–13.
45) M. Mongy: Nuovo Cim. **8** (1972) 247–255.
46) A. Seeger: Philos. Mag. Lett. **83** (2003) 107–115.
47) M. Weller, J. Diehl and W. Mensch: Phys. Status Solidi **60** (1980) 93–101 (a).
48) W. Frank, A. Seeger and M. Weller: Radiat. Eff. **55** (1981) 111–118.
49) H.M. Simpson and A. Sosin: Phys. Rev. B **5** (1972) 1382–1393.
50) H.M. Simpson and A. Sosin: Phys. Rev. B **16** (1977) 1489–1494.